Noise, Large-Signal Modeling and Characterization of InP/InGaAs HBTs

N. Lal, S. Nuttinck, A. Raghavan, E. Gebara*, S. Venkataraman, J. Papapolymerou and J. Laskar

School of Electrical and Computer Engineering, Georgia Institute of Technology, Atlanta, GA 30332, neeraj@ece.gatech.edu
*Quellan Inc., 250 14th Street NW, Atlanta, GA 30318, edward@quellan.com

ABSTRACT -- We developed a robust large-signal model for InP/InGaAs HBTs. DC, small-signal, noise and power characteristics of InP/InGaAs HBTs are measured over a wide range of frequencies and bias conditions. A minimum noise figure (F_{MIN}) of 3.5dB, and a gain of 16.8dB are achieved at 10-GHz. These measurement results are the basis for robust nonlinear models of InP/InGaAs HBT devices.

I. INTRODUCTION

As technology advances and the world increasingly adopts faster network connections and higher frequency applications, it is necessary to migrate to a device technology capable of handling these requirements. Indium Phosphide (InP) has proven to be one of these technologies that will be able to handle the increased bandwidth and high frequency applications with relative ease, Chen et al (1) and Kobayashi et al (2).

Superior electron transport for high speed, low turn-on voltage for low power ICs, reduced 1/f noise, improved thermal conductivity, reduced surface recombination, small base-emitter turn-on voltage, high electron mobility and the potential for optoelectronic integration are the drivers for the development of InP-based HBT technology, Hu and Pavlidis (3), Wong and Ing Ng (4).

While extensive and thorough characterization has been performed on the InP HEMT process, development of models for InP-based HBTs is still in its early stages. These models are crucial in order to provide ICs with performances that can compete with more mature technologies such as InP-based HEMT and SiGe-based HBT. Integration of both noise and nonlinear behavior is a requirement for accurate circuit simulations.

In this paper we have presented the complete comprehensive characterization of InP/InGaAs HBTs over a wide range of frequencies and bias conditions. These measurements are the basis for the robust development of an accurate large-signal model.

II. DEVICE CHARACTERIZATION

The device measured was fabricated in a mesa isolated self aligned standard heterojunction bipolar transistor (HBT) process. The HBTs are composed of an InP emitter with an InGaAs base.

The device under analysis is a single-emitter device having the dimensions of 1.6x1x6.8μm^2. This device has been characterized up to 45-GHz. Fig. 1 shows a picture of measured InP/InGaAs HBTs.

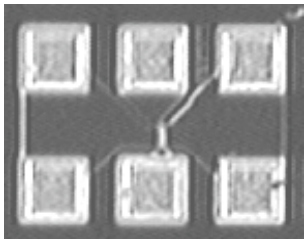

Fig. 1 Photograph of the InP/InGaAs HBT device

The device exhibits a measured cutoff frequency (f_T) above 150-GHz as well as a maximum frequency of oscillation (f_{MAX}) beyond 150-GHz. Fig. 2 shows the characterization of the HBT with I_C vs. I_B and I_B vs. f_T.

Power and noise characterization of these devices are performed over a complete range of bias values and frequency points. The noise parameters have been extracted using an ATN/Agilent noise measurement system up to 22-GHz. Fig. 3 shows the minimum noise figure (F_{MIN}) at three different bias conditions. Our measurements show that F_{MIN} decreases with a decrease in the base current (I_B) as well as the collector current (I_C). A F_{MIN} value of 3dB was measured. This relatively

large value of F_{MIN} is attributed to the high input base resistance of the devices.

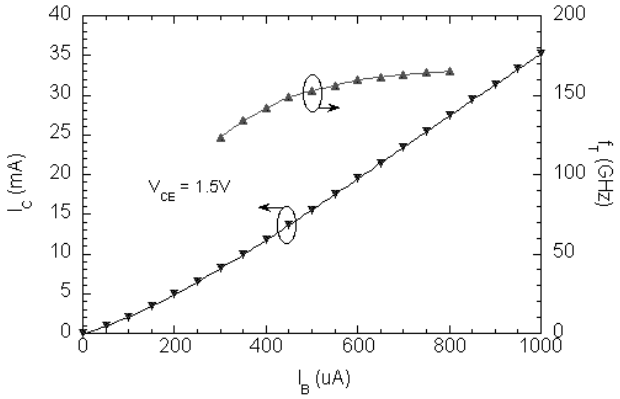

Fig. 2 I_C vs. I_B and f_T vs. I_B for the HBT device

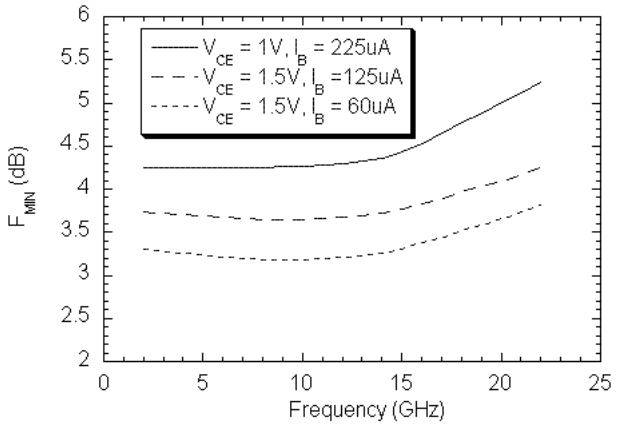

Fig. 3 F_{MIN} versus frequency at 3 different bias conditions

The power characteristics were measured using an ATN/Agilent load-pull system. Performances are measured at 10-GHz, with the tuning of the load and source impedances performed for maximum output power at the 1dB compression point. Fig. 4 shows measurement results obtained for the gain and the output power versus input power. The collector-to-emitter

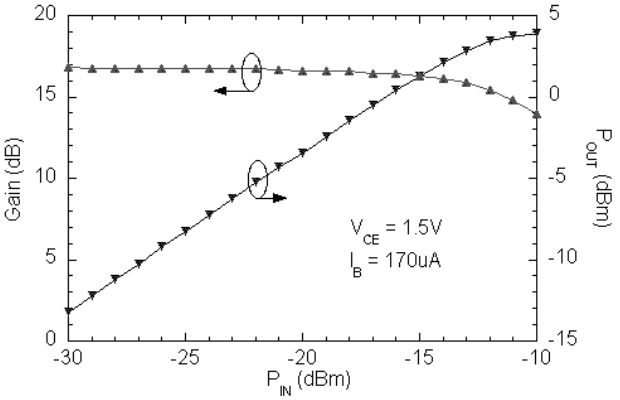

Fig. 4 Power sweep and gain results at a fixed collector current density of 0.5mA/□m^2 and a base current of 170□A

voltage (V_{CE}) is fixed at 1.5V while a base current (I_B) 0f 170□A was selected to achieve a collector current density of 0.5□A/□m^2. This current is well within the linear range of the device and resulted in an overall gain of the device of 16.8dB.

Table1 summarizes the RF performances and characterization of the InP/InGaAs HBT at 10-GHz at three different bias conditions.

Bias	**V_{CE}=1V I_B=225□A**	**V_{CE}=1.5V I_B=125□A**	**V_{CE}=1.5V I_B=60□A**
I_C (m□)	6	3	1
F_{MIN} (dB)	4.2	3.6	3.1
R_N (□)	77	82	93
Gain (dB)	13.8	16.8	12.1
P_{out}^{1dB} (dBm)	0.8	2.8	-3.9

Table 1 RF performance summary of the InP/InGaAs HBT

III. LARGE-SIGNAL MODELING

A number of large-signal models have been proposed by a variety of people. These models include the Spice Gummel-Poon model (GHP), Yang et al (5); the VBIC model, McAndrew et al (6); the HICUM model, Schroter et al (7); and the MEXTRAM model, de Graff et al (8).

All of these proposed models listed above are all physics-based models. The problem with these physics-based models is that they require the extraction of a large number of parameters and the knowledge of the corresponding process parameters.

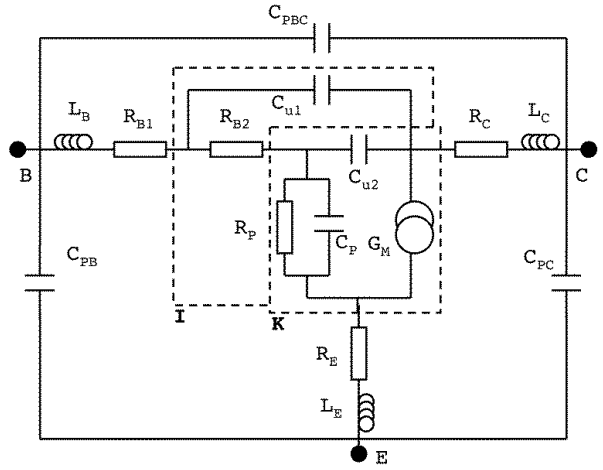

Fig. 5 Small-signal equivalent hybrid-□ circuit model for the InP/InGaAs HBT.

This section examines the physics-based empirical model for HBT devices. We model the behavior of an InP/InGaAs HBT at various bias conditions from DC to

40-Ghz using the hybrid-Pi equivalent circuit model as shown in Fig. 5.

This model can be divided into three parts: the parasitic elements (L_B, L_C, L_E, R_{B1}, R_C, R_E, C_{PB}, C_{PC}, C_{PBC}), the feed-back network elements (R_{B2}, C_{u1})), and the kernel elements (R_P, C_P, C_{u2}, G_M).

The parasitic elements are extracted using the conventional Cold-method of measurements developed by Gobert et al (9). The elements of the feedback network and of the kernel are determined using a combination of Suh et al (10) and Costa et al's (11) methodology. The final element values have been determined through an optimization procedure with a CAD tool. The resulting values obtained for the parasitic elements are listed in Table 2.

L_B	14 pH	C_P	10 fF	R_{B1}	11 Ω
L_E	60 pH	C_{PBC}	20 fF	R_E	1 Ω
L_C	150 pH	C_{u1}	20 fF	R_C	60 Ω
C_{PC}	50 fF	C_{u2}	11 fF	R_{B2}	11 Ω
C_{PB}	38 fF	G_M	150 mS	R_P	250 Ω

Table 2 Extracted parameters for the small-signal model of the InP/InGaAs HBT @ I_B=300μA, I_C=8.2mA, and V_{CE}=1.5V

The measured and modeled S-parameters of the InP/InGaAs HBT device are shown in Fig. 6, from DC to 40-GHz.

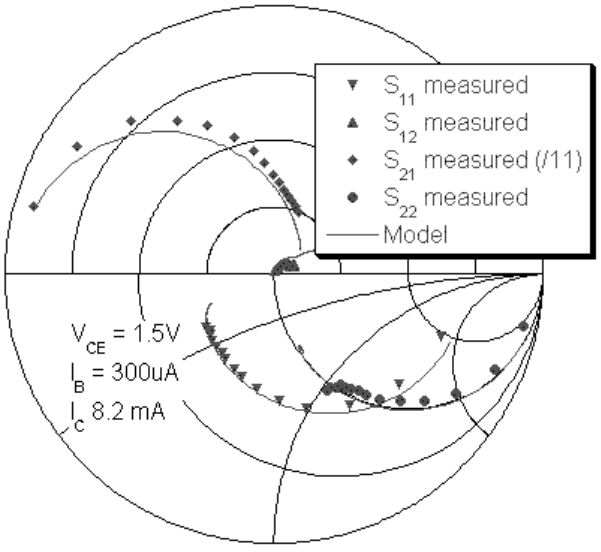

Fig. 6 Modeled and measured S-parameters from DC to 40GHz of an InP/InGaAs HBT.

Also, in applications where f_T is well above the frequency of operation, the device current-voltage characteristics dominates its nonlinear behavior, thus making the modeling of the current source critical for accurate large-signal simulation. Precise extraction of the total base resistance ($R_{BTOT} = R_{B1}+R_{B2}$) is crucial for internal current source modeling purposes. The analytical expression in Eqn.1 developed by Suh et al(12), shows a method for calculation of the total base resistance valid at high frequencies.

$$R_{btot} = \mathrm{Re}\left[\tilde{z}_{11} - \tilde{z}_{12}\frac{\tilde{z}_{12} - \tilde{z}_{21}}{\tilde{z}_{22} - \tilde{z}_{12}}\right] \qquad \text{Eqn.1}$$

where z_{ij} refers to the z-parameters after the de-embedding of the parasitic inductive and capacitive elements.

Fig. 7 shows good agreement between the measured and modeled current-voltage characteristics of the InP/InGaAs HBT. The large-signal model is developed from the DC-IV and bias dependent small-signal modeling results.

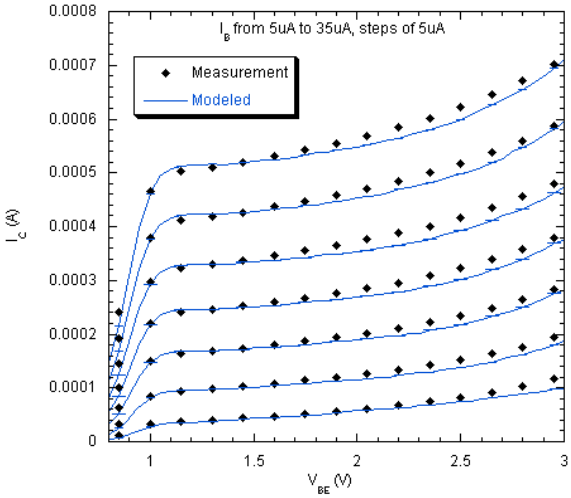

Fig. 7 Modeled and measured HBT current-voltage characteristics.

IV. CONCLUSION

The measurements for noise and power have been made on InP HBT devices and additionally, large-signal modeling using physics-based empirical models for HBT devices have been presented. The validity of the model has been shown through the comparison with the measured s-parameter of the circuit. The work presented here is the first such combination of noise, power and large-signal measurements and models on Indium Phosphide HBT devices that is known to the authors.

ACKNOWLEDGEMENT

The authors wish to acknowledge Lee Wiederspahn and Vitesse Semiconductor for their collaboration effort as well as the devices for the modeling and measurement. The authors would also like to acknowledge the

Yamacraw Design Center for their support in the development of this project.

REFERENCES

(1) Y.K. Chen, D.A. Humphrey, L. Fan, J. Lin, R.A. Hamm, D. Sivco, A.Y. Cho, and A. Tate. "Noise Characteristics of InP-based HBTs," *Indium Phosphide and Related Materials,* pp. 851-856, 1995.

(2) K. W. Kobayashi, J. Cowles, L. T. Tran, A. Gutierrez-Aitken, T. R. Block, A. K. Oki and D. C.Streit. "A 50-MHz-55-GHz multidecade InP-based HBT distributed amplifier," *IEEE Microwave Guided Wave Letters,* vol.7, pp. 353-355, Oct. 1997.

(3) S. H. Hu and D. Pavlidis. "Low Noise, High-Speed InP/InGaAs HBTs." *GaAs IC Symposium Technical Digest,* pp. 188-191, 2001.

(4) H. Wong and G. Ing Ng. "Electrical Properties and Transport Mechanisms of InP/InGaAs HBTs Operated at Low Temperature," *IEEE Transactions on Electron Devices,* vol. 48, no. 8, pp. 1492-1497, August 2001.

(5) K. Yang, A.L. Gutierrez-Aitken, X. Zhang, P. Bhattacharya, and G.I. Haddad. "An HSPICE HBT Model for InP-Based Single HBT's," *IEEE Transactions on Electron Devices,* vol. 43, no. 9, pp. 1470-1472, 1996.

(6) C. McAndrew, J. Seitchik, D. Bowers, M. Dunn, M. Foisy, I. Getreu, M. McSwain, S. Moinian, J. Parker, P. van Wijnen, and L. Wagner. "VBIC95: An Improved vertical, IC bipolar transistor model," *Proceedings of the Bipolar/BiCMOS Circuits and Technology Meeting,* pp. 170-177, 1995.

(7) M. Schroter, H.-M. Rein, R. Reimann, H.-J. Wassener, and A. Koldehoff. "Physics and process-based bipolar transistor modeling for integrated circuit design," *IEEE Journal of Solid State Circuits,* vol. 34, no. 8, pp. 1136-1149, 1999.

(8) H.C. de Graaff, W.J. Kloosterman, J.A.M. Gleelan, M.C.A.M Koolen. "Experience with the new compact MEXTRAM model for bipolar transistors," Proceedings *of the Bipolar Circuits and Technology Meeting,* pp. 246-249, 1989.

(9) Y. Gobert, P. J. Tasker, and K. H. Bachem. "A Physical, Yet Simple, Small-Signal Equivalent Circuit for the Heterojunction Bipolar Transistor," *IEEE Transactions on Microwave Theory and Techniques,* vol. 45, no. 1, pp. 149-153, 1997.

(10) Y. Suh, E. Seok, J.-H. Shin, B. Kim, D. Heo, A. Raghavan, J. Laskar. "Direct Extraction Method for Internal Equivalent Circuit Parameters of HBT Small-Signal Hybrid-π Model," *IEEE MTT-S 2000 IMS Symposium Digest,* pp. 1401-1404, 2000.

(11) D. Costa, W. Liu, and J. S. Harris. "Direct Extraction of the AlGaAs/GaAs Heterojunction Bipolar Transistor Small-Signal Equivalent Circuit," *IEEE Trans. On Electron Devices,* vol. 38, no. 9, pp. 2018-2024, 1991.

(12) Y. Suh, D. Heo, A. Raghavan, E. Gebara, S. Nuttnick, K. Lim and J. Laskar, "Direct Extraction and Modeling Method for Temperature Dependent Large Signal CAD Model of Si-BJT", *IEEE MTT-S 2001 IMS Symposium Digest,* pp. 971-974, 2001.